

Measurement of Beta Decay Properties of Nuclei of Interest for Nuclear Structure and Astrophysics, and Applications

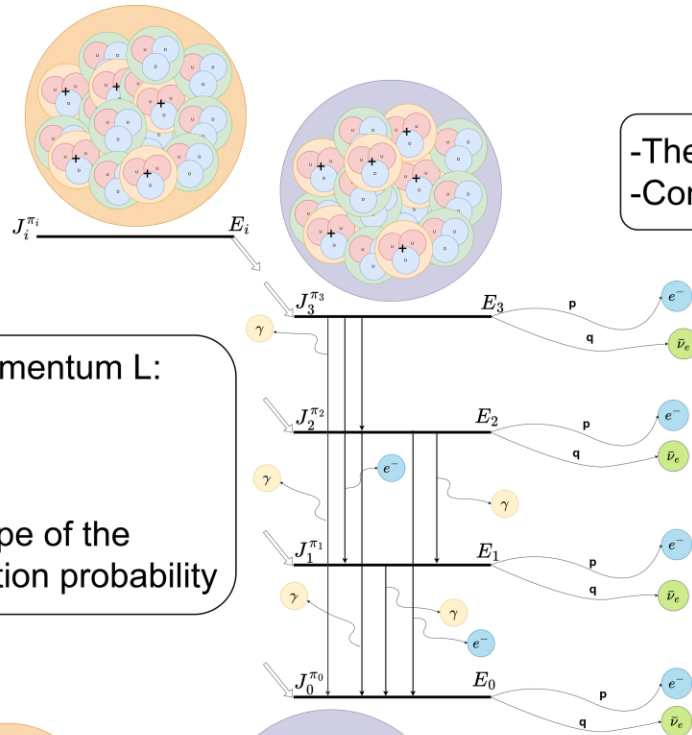
PhD Hour – DURAND Samuel

Supervisors :
ESTIENNE Magali,
FALLOT Muriel

Outline

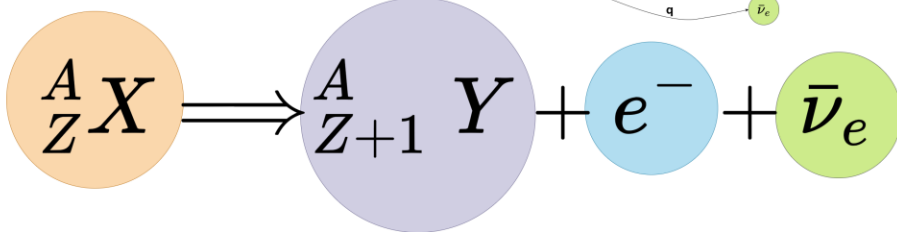
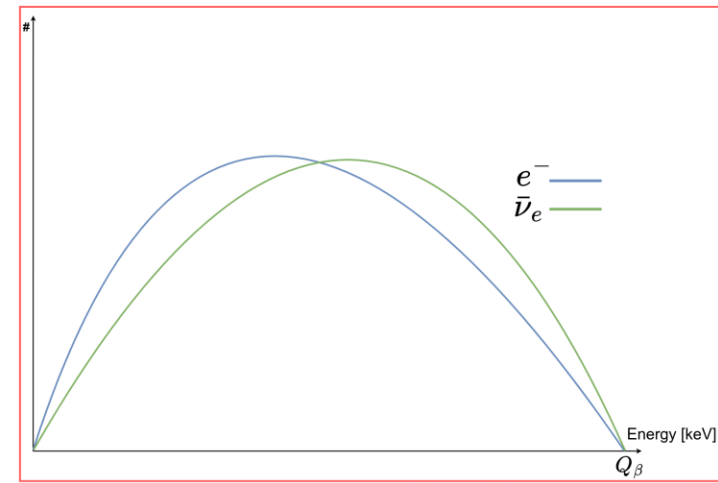
- Beta decay properties
- Physics motivations
- The e-Shape Experiment
- Detector and Geant4 Geometry
- Detector Calibration
- Data-Simulation Comparison
- Conclusions and Outlooks

Beta decay properties



-The available decay energy, called Q-value, is shared between the emitted leptons
 -Continuous energy spectra for the emitted particles.

The leptons carry an angular momentum L:
-Allowed transition
 $\Delta L = 0$
-Forbidden transition
 $\Delta L \neq 0$ -> modification of the shape of the spectrum, reduction of the transition probability



- Unlike allowed transitions, forbidden decays are much less understood
 - Their accurate description remains a major challenge.

Beta decay properties

Electron energy distribution

$$N_e(p) \approx p^2(Q - T_e)^2 F(Z', p) |M_{fi}^a|^2 S(p, q) (1 + \delta(Z, A, p))$$

Phase space

$$p^2(Q - T_e)^2$$

Kinematic term predicted by Fermi's theory

Fermi function

$$F(Z', p)$$

Coulomb correction between the emitted electron and the daughter nucleus

Allowed nuclear matrix element

$$|M_{fi}^a|^2$$

Energy-Independent nuclear transition strength used for allowed approximation

My analysis focus

Shape factor

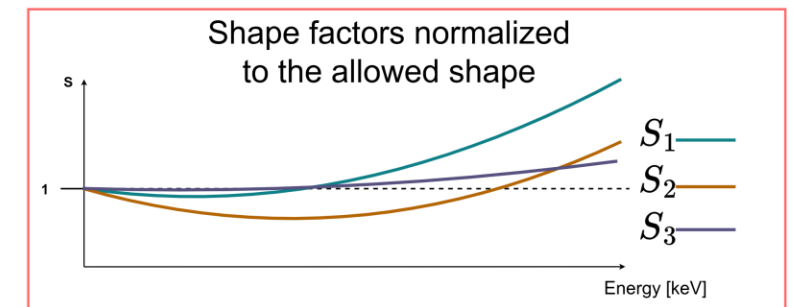
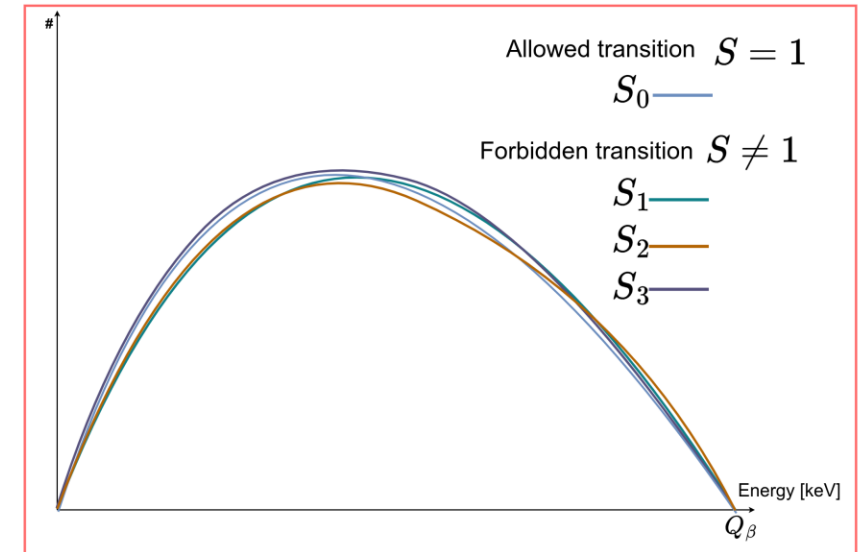
$$S(p, q)$$

Energy-dependent nuclear transition strength term accounting for nuclear structure effects beyond the allowed approximation

Quantum corrections

$$1 + \delta(Z, A, p)$$

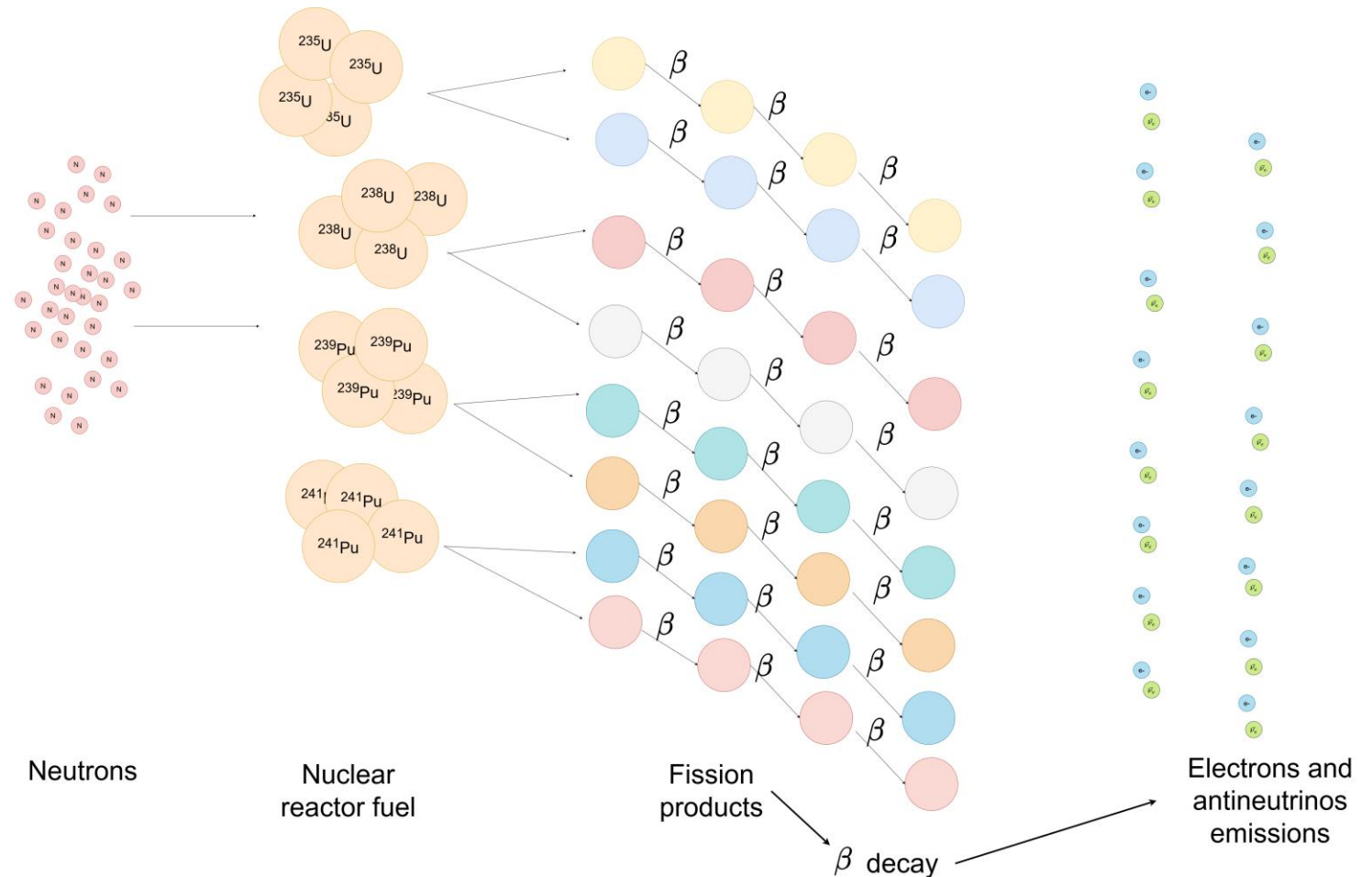
Higher-order corrections, including radiative, finite-size, screening, recoil, and weak-magnetism effects



Physics motivations

Reactor antineutrino spectra prediction: introduction

- Reactor antineutrino spectra originate from the beta decay of hundreds of fission fragments in the reactor core
- Their prediction requires combining nuclear structure and decay data: fission yields, branching ratios and beta spectra
- The spectral shape reflects detailed nuclear structure
- Accurate predictions are essential inputs for reactor neutrino experiments and oscillation measurements



Physics motivations

Reactor antineutrino spectra prediction: methods

Conversion method

- Fit of effective beta spectra decomposed into virtual branches to reproduce ILL integral beta spectrum measurements (1980s), converted into antineutrino spectra using beta decay theory
- Weak dependence on nuclear decay data, but subject to modeling biases in the conversion method (virtual β branches, fitting procedure)

Summation method

- Builds the spectrum by summing β -decay branches of fission products, weighted by fission yields and branching ratios
- Predictive and flexible but can be limited by nuclear data uncertainties

Diagram illustrating the summation method equation:

$$S_{fp}(E) = \sum_{b=1}^{N_b} I_{\beta}^b * S_{fp}^b(Z_{fp}, A_{fp}, E_{0fp}^b, E)$$

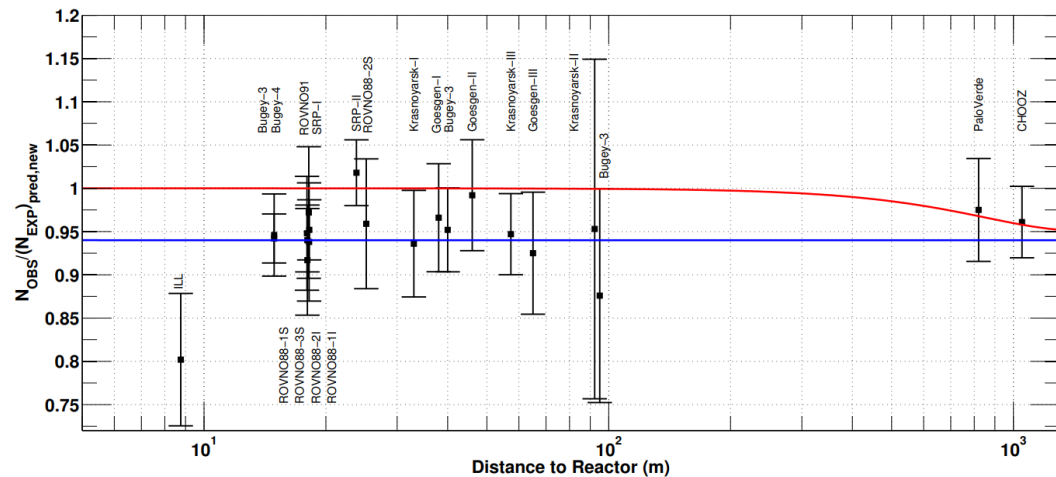
The diagram shows three labels with arrows pointing to the equation: 'Total fission product spectrum' points to the left side of the equation, 'Branching ratio' points to the I_{β}^b term, and 'Branch spectrum' points to the S_{fp}^b term.

Physics motivations

Reactor antineutrino spectra prediction: anomalies

Reactor antineutrino anomaly (RAA)

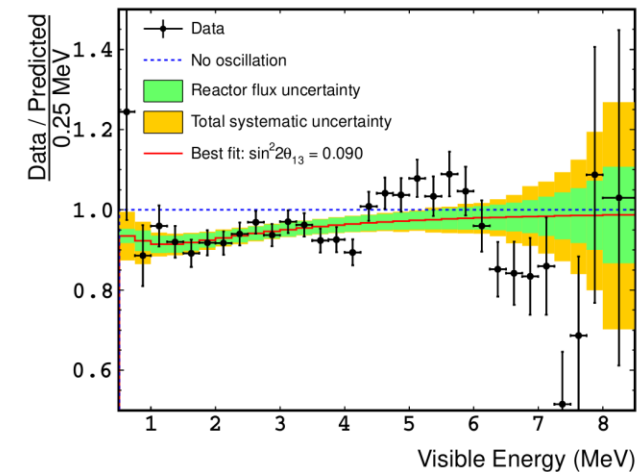
- Re-evaluation of reactor antineutrino flux predictions increased the expected flux (Huber-Mueller 2011)
- Short-baseline reactor experiments antineutrino flux measurements deficit of 6% when compared to predictions
- Possible origins : nuclear physics, experimental systematics, or new neutrino physics



G. Mention et al. Phys. Rev. D83, 073006 (2011)

Shape anomaly

- Distortion of the measured antineutrino energy spectrum relative to predictions
- Excess of events observed ($\sim 10\%$) around 5-7MeV antineutrino energy reported by multiple reactor experiments (Daya Bay, RENO, Double Chooz)
- Suggests deficiencies in reactor spectrum modeling and/or nuclear data (shape factors are a leading hypothesis)



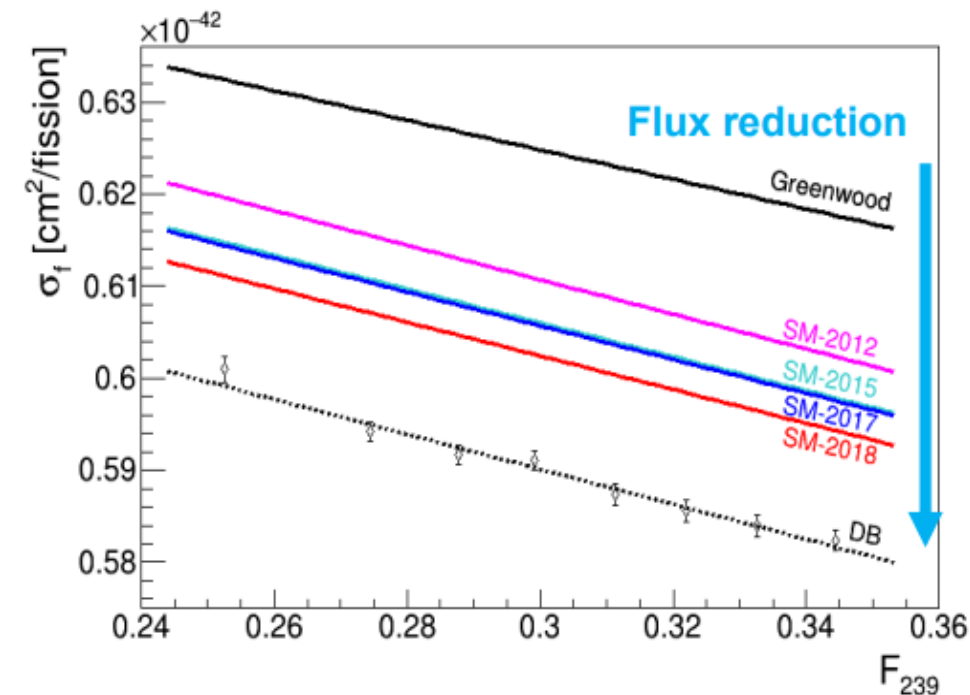
Y. Abe et al. (Double Chooz Collaboration), J. High Energy Phys. 10 (2014) 086; 02 (2015) 74

Physics motivations

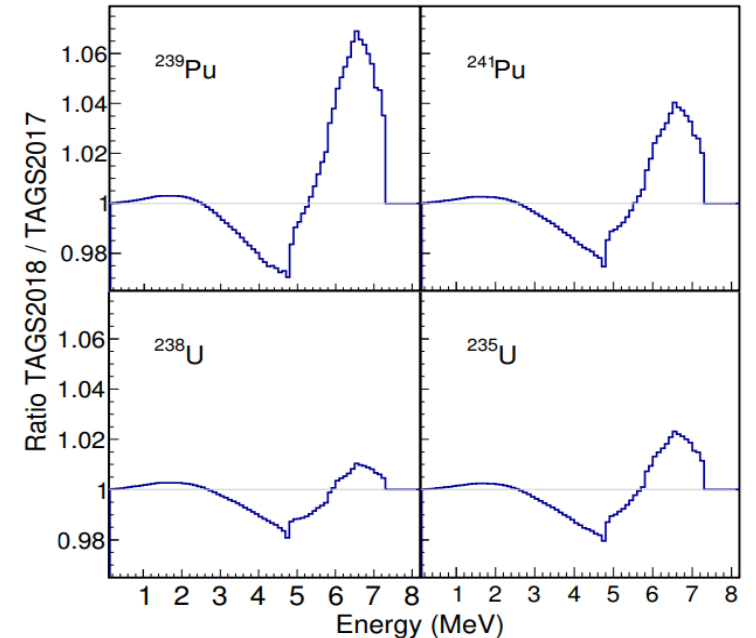
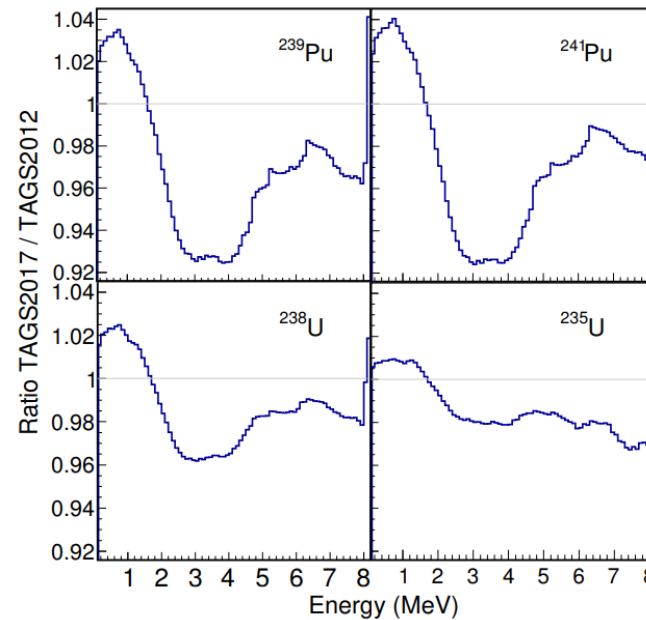
Reactor antineutrino spectra prediction: anomalies status

Reactor antineutrino anomaly (RAA)

- The summation method has been strongly improved over the years along with nuclear data and is now more predictive than the conversion method
- The antineutrino flux prediction improved with TAGS data being included (~1% discrepancy)



M. Estienne et al., Phys. Rev. Lett. 123 (2019) 022502



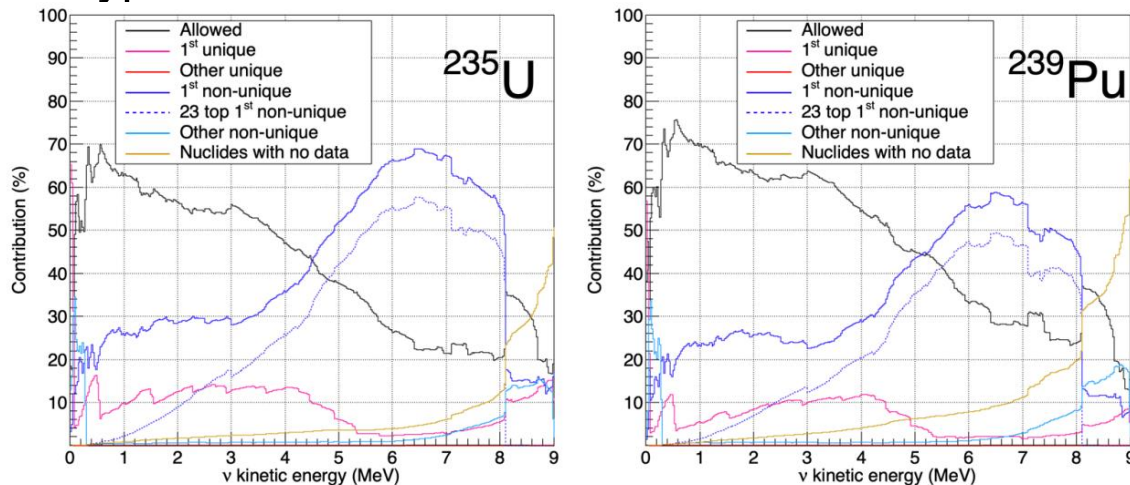
Algora, A., Tain, J.L., Rubio, B., Fallot, M., Gelletly, W. Beta-decay studies for applied and basic nuclear physics. *Eur. Phys. J. A* **57**, 85 (2021)

Physics motivations

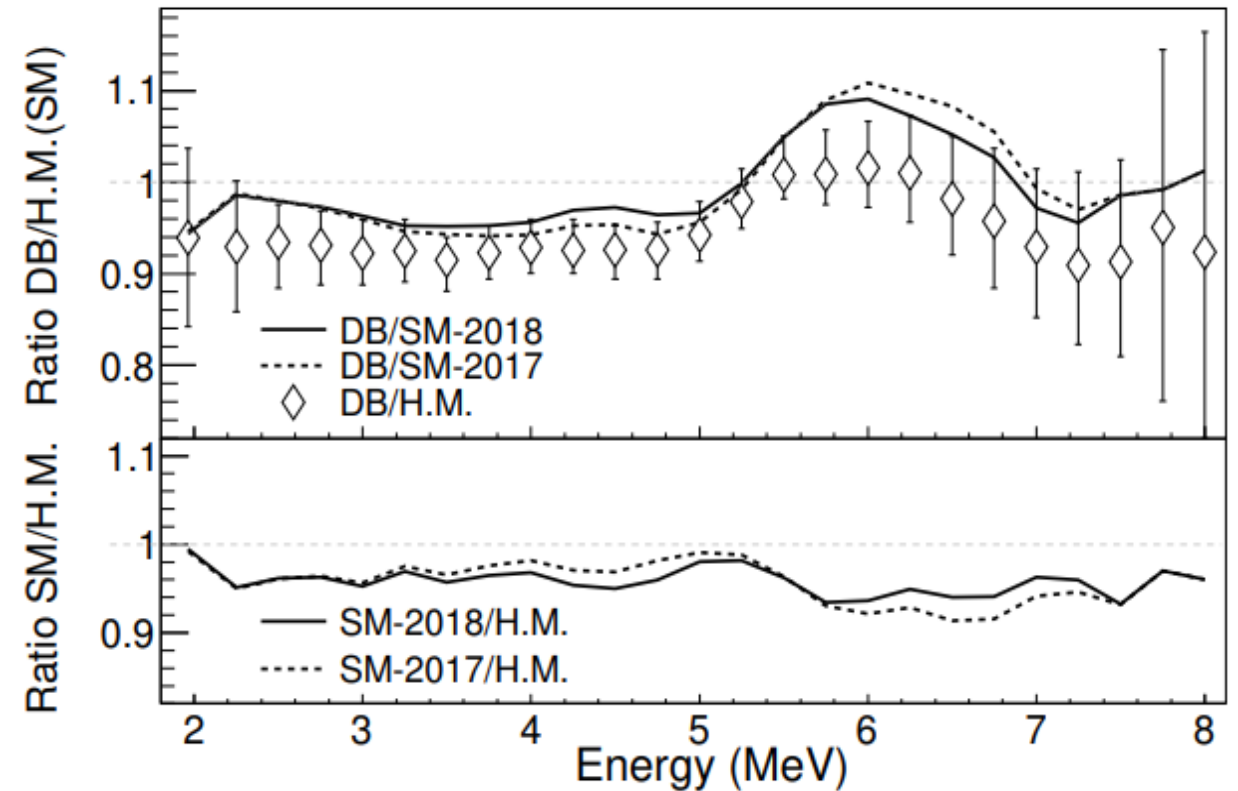
Reactor antineutrino spectra prediction: anomalies status

Shape anomaly

- Both prediction methods still observe the shape anomaly and its origin is still unknown
- Need experimental data to validate or refute the various hypotheses to explain this anomaly
- Forbidden transition shape factors are a leading hypothesis



L. Perissé et al., Phys. Rev. C 108 (2023), 055501



M. Estienne et al., Phys. Rev. Lett. 123 (2019) 022502

Physics motivations

Reactor antineutrino spectra prediction: physics cases

- Physics cases for my PhD:
- ⁹⁶Y: small shape factor prediction, high contribution to the spectra
- ⁹⁴Y: large shape factor prediction, moderate contribution to the spectra

TABLE I. Main contributors to a standard PWR antineutrino energy spectrum computed with the MURE code coupled with the list of nuclear data given in [12] and assuming that they have been emitted by ²³⁵U (52%), ²³⁹Pu (33%), ²⁴¹Pu (6%) and ²³⁸U (8.7%) for a 450 day irradiation time, and using the summation method described in [12].

	4 - 5 MeV	5 - 6 MeV	6 - 7 MeV	7 - 8 MeV
⁹² Rb	4.74%	11.49%	24.27%	37.98%
⁹⁶ Y	5.56%	10.75%	14.10%	-
¹⁴² Cs	3.35%	6.02%	7.93%	3.52%
¹⁰⁰ Nb	5.52%	6.03%	-	-
⁹³ Rb	2.34%	4.17%	6.78%	4.21%
^{98m} Y	2.43%	3.16%	4.57%	4.95%
¹³⁵ Te	4.01%	3.58%	-	-
^{104m} Nb	0.72%	1.82%	4.15%	7.76%
⁹⁰ Rb	1.90%	2.59%	1.40%	-
⁹⁵ Sr	2.65%	2.96%	-	-
⁹⁴ Rb	1.32%	2.06%	2.84%	3.96%

Zakari-Issoufou et al. PRL 115.102503(2015)

Table I. Dominant forbidden transitions above 4 MeV. Here Q_{β} is the ground-state to ground-state Q -value, E_{ex} the excitation energy of the daughter level, BR the branching ratio of the transition normalized to one decay and FY the cumulative fission yield of ²³⁵U from the ENDF database [43]. Transitions with small fission yields shown here contribute substantially more for ²³⁸U and ²⁴¹Pu.

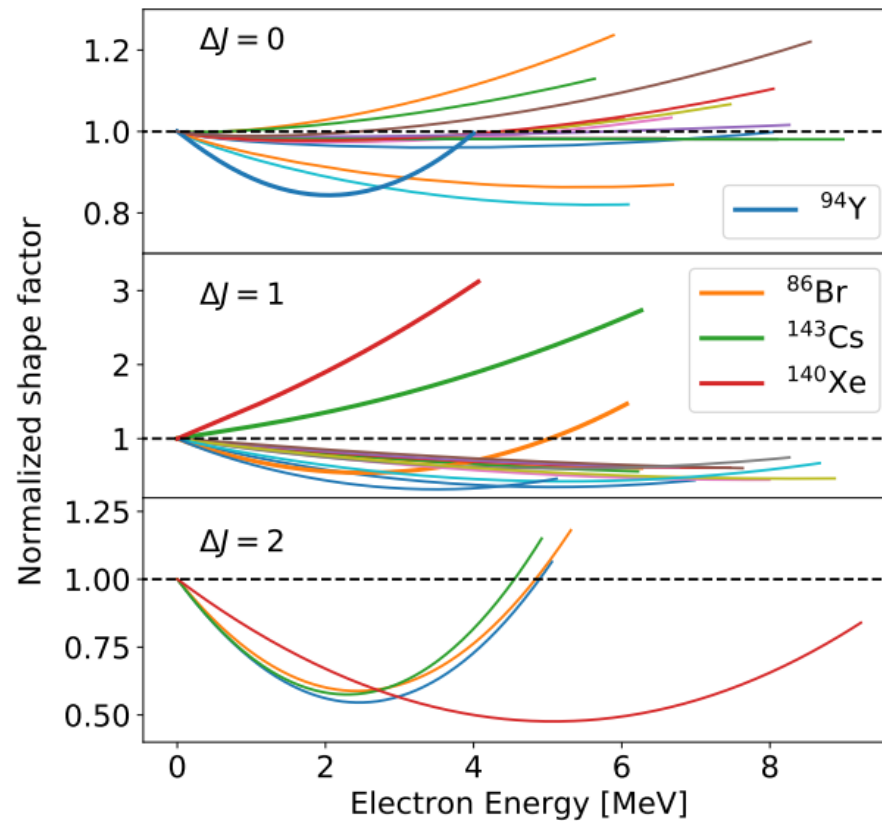
Nuclide	Q_{β} (MeV)	E_{ex} (MeV)	BR (%)	$J_i^{\pi} \rightarrow J_f^{\pi}$	FY (%)	ΔJ
⁸⁹ Br	8.3	0	16	3/2 ⁻ → 3/2 ⁺	1.1	0
⁹⁰ Rb	6.6	0	33	0 ⁻ → 0 ⁺	4.5	0
⁹¹ Kr	6.8	0.11	18	5/2 ⁺ → 5/2 ⁻	3.5	0
⁹² Rb	8.1	0	95.2	0 ⁻ → 0 ⁺	4.8	0
⁹³ Rb	7.5	0	35	5/2 ⁻ → 5/2 ⁺	3.5	0
⁹⁴ Y	4.9	0.92	39.6	2 ⁻ → 2 ⁺	6.5	0
⁹⁶ Rb	9.3	0.68	5.9	5/2 ⁻ → 5/2 ⁺	1.7	0
⁹⁵ Sr	6.1	0	56	1/2 ⁺ → 1/2 ⁻	5.3	0
⁹⁶ Y	7.1	0	95.5	0 ⁻ → 0 ⁺	6.0	0
⁹⁷ Y	6.8	0	40	1/2 ⁻ → 1/2 ⁺	4.9	0
⁹⁸ Y	9.0	0	18	0 ⁻ → 0 ⁺	1.9	0
¹³³ Sn	8.0	0	85	7/2 ⁻ → 7/2 ⁺	0.1	0
¹³⁵ Te	5.9	0	62	(7/2 ⁻) → 7/2 ⁺	3.3	0
¹³⁵ Sb	8.1	0	47	(7/2 ⁺) → (7/2 ⁻)	0.1	0
^{136m} I	7.5	1.89	71	(6 ⁻) → 6 ⁺	1.3	0
^{136m} I	7.5	2.26	13.4	(6 ⁻) → 6 ⁺	1.3	0
¹³⁷ I	6.0	0	45.2	7/2 ⁺ → 7/2 ⁻	3.1	0
¹⁴² Cs	7.3	0	56	0 ⁻ → 0 ⁺	2.7	0
⁸⁶ Br	7.3	0	15	(1 ⁻) → 0 ⁺	1.6	1
⁸⁶ Br	7.3	1.6	13	(1 ⁻) → 2 ⁺	1.6	1
⁸⁷ Se	7.5	0	32	3/2 ⁺ → 5/2 ⁻	0.8	1
⁸⁹ Br	8.3	0.03	16	3/2 ⁻ → 5/2 ⁺	1.1	1
⁹¹ Kr	6.8	0	9	5/2 ⁺ → 3/2 ⁻	3.4	1
⁹⁵ Rb [†]	9.3	0.56	6.0	5/2 ⁻ → (7/2 ⁺)	1.7	1
⁹⁵ Rb	9.3	0.68	5.9	5/2 ⁻ → 3/2 ⁺	1.7	1
^{134m} Sb	8.5	1.69	42	(7 ⁻) → 6 ⁺	0.8	1
^{134m} Sb	8.5	2.40	54	(7 ⁻) → (6 ⁺)	0.8	1
¹³⁶ Te	5.1	0	8.7	0 ⁺ → (1 ⁻)	3.7	1
¹³⁸ I	8.0	0	26	(1 ⁻) → 0 ⁺	1.5	1
¹⁴⁰ Xe	4.0	0.08	8.7	0 ⁺ → 1 ⁻	4.9	1
¹⁴⁰ Cs	6.2	0	36	1 ⁻ → 0 ⁺	5.7	1
¹⁴³ Cs	6.3	0	25	3/2 ⁺ → 5/2 ⁻	1.5	1
⁸⁸ Rb	5.2	0	76.5	2 ⁻ → 0 ⁺	3.6	2
⁹⁴ Y	4.9	0	41	2 ⁻ → 0 ⁺	6.5	2
⁹⁶ Rb	9.3	0	0.1	5/2 ⁻ → 1/2 ⁺	1.7	2
¹³⁹ Xe	5.1	0	15	3/2 ⁻ → 7/2 ⁺	5.0	2

Physics motivations

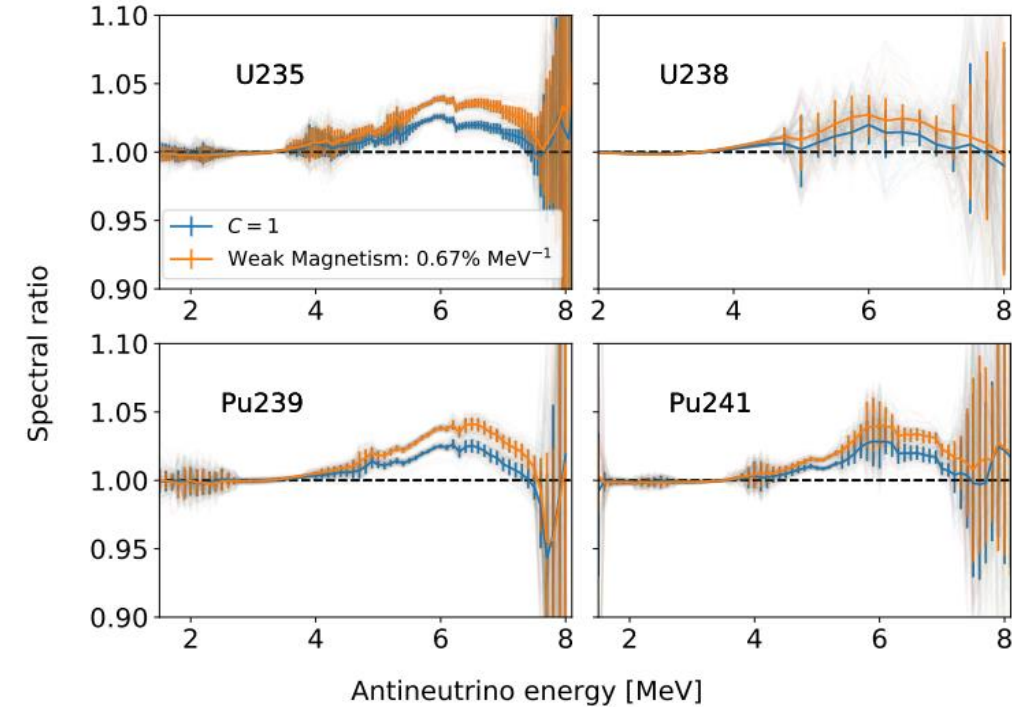
Reactor antineutrino spectra prediction: physics cases

Physics cases for my PhD:
 - ^{96}Y : small shape factor prediction, high contribution to the spectra
 - ^{94}Y : large shape factor prediction, low contribution to the spectra

Shape factors prediction

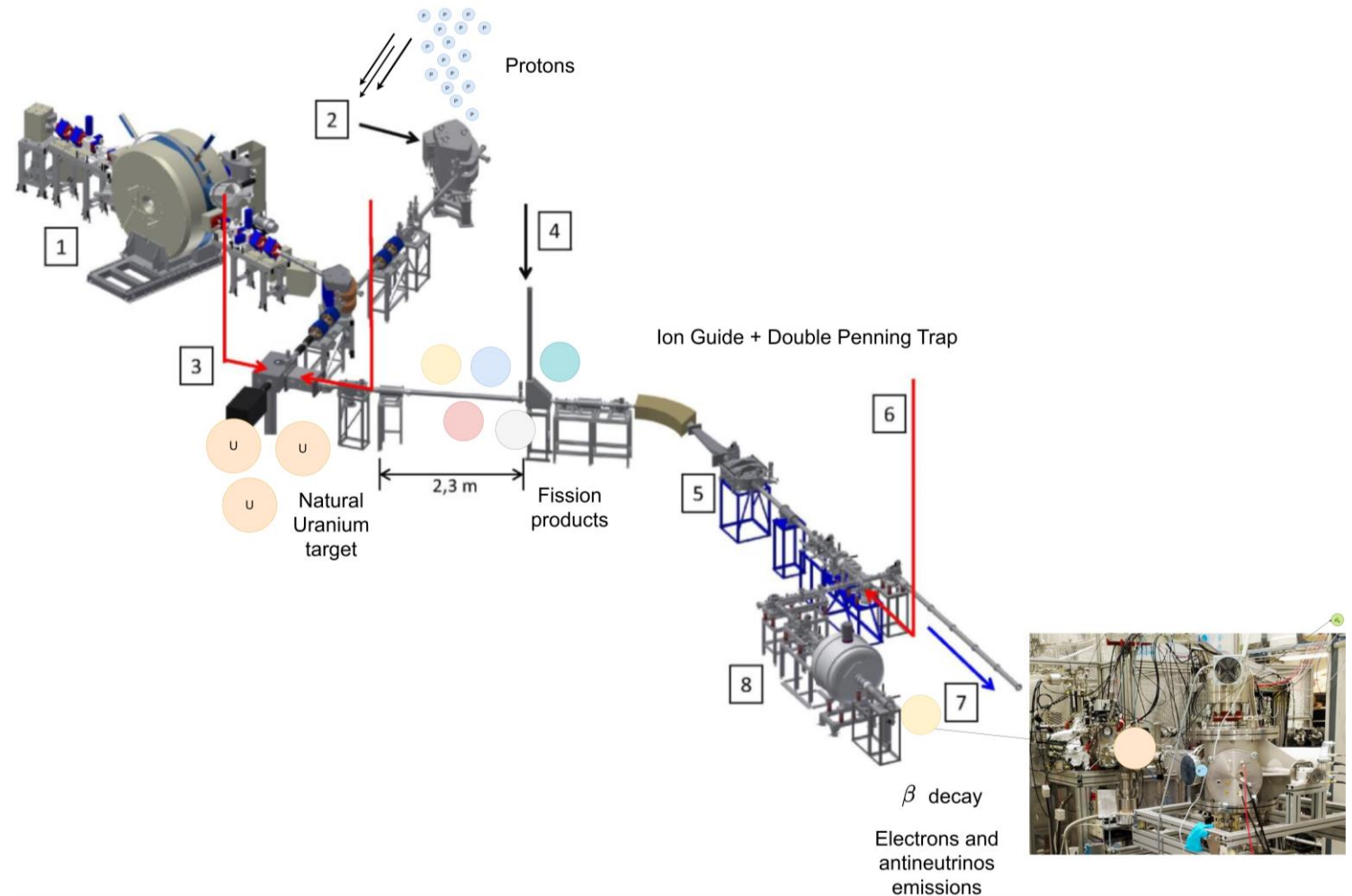


Ratio of antineutrino spectra predicted with and without those shape factors



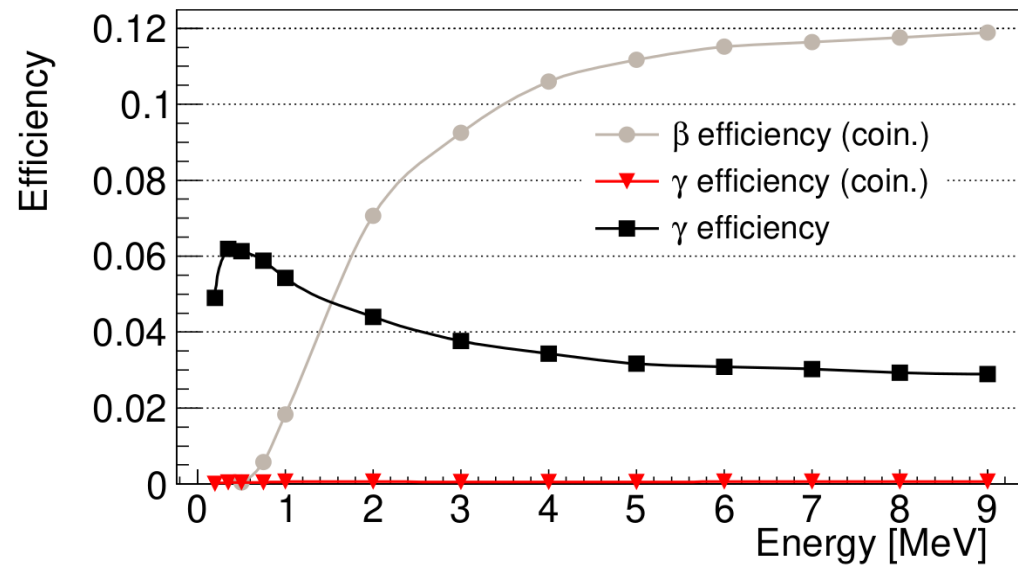
The e-Shape experiment

- Jyväskylä, Finland, IGISOL-4
- 2 experimental campaigns (2022, 2023)
- Dozen measured nuclei of interest in the 2nd campaign

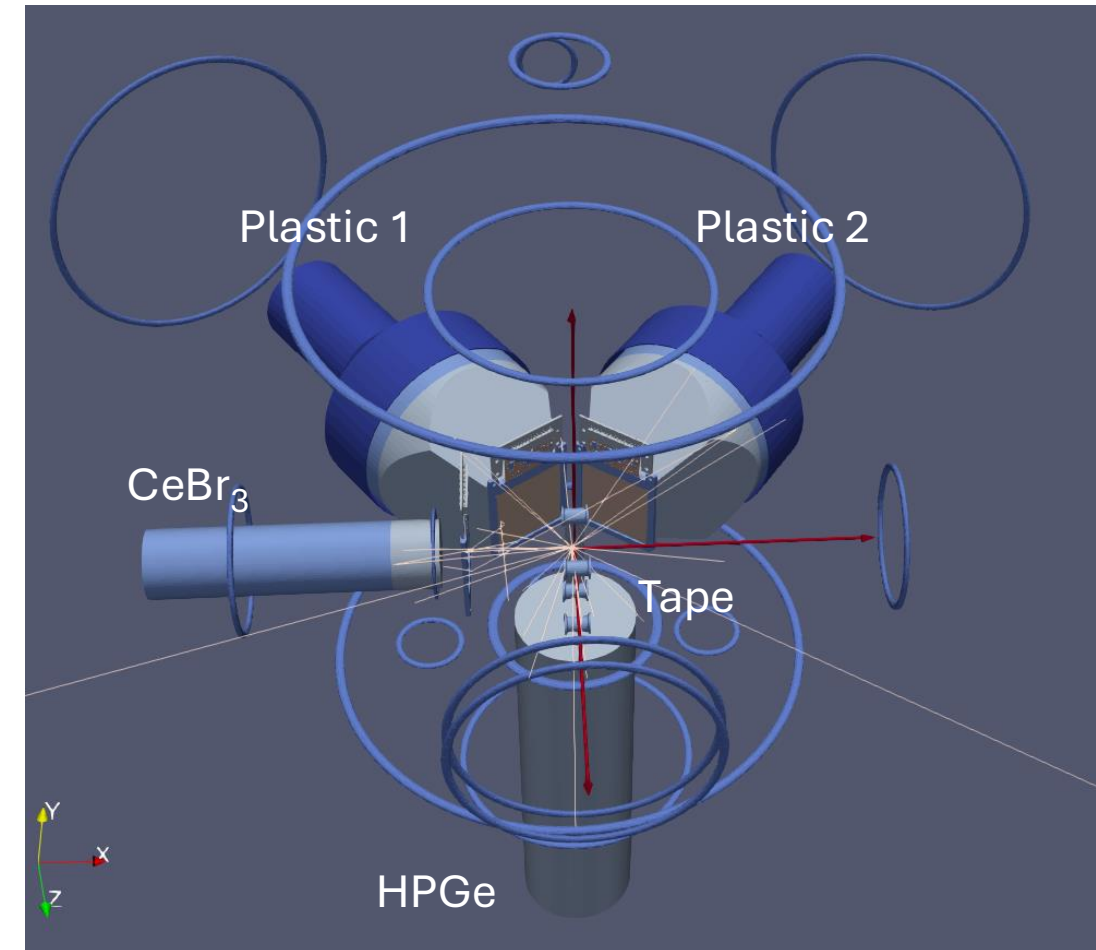


Detector and GEANT4 geometry

- 3 Telescopes + 1 HPGe
- Telescope : Scintillator (plastic or CeBr_3) + Semiconductor (300 μm silicon for plastic telescopes and 500 μm for CeBr_3 telescope)
- Coincidence : subtraction of most of the gamma spectrum
- For data acquisition, FASTER electronics (LPC Caen, France) was used



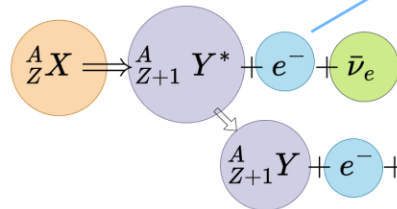
V. Guadilla et al 2024 JINST 19 P02027



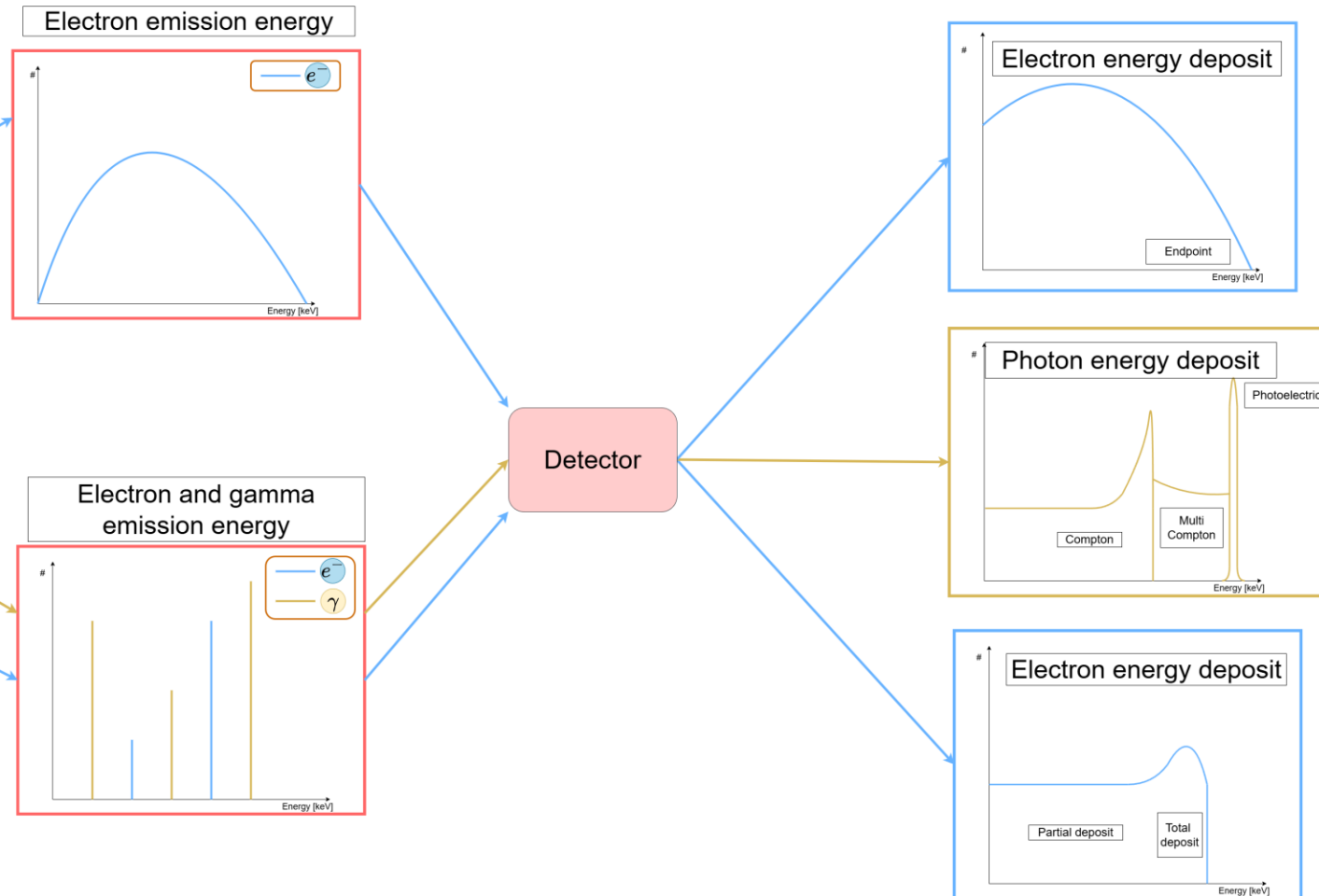
Detectors calibration

Calibration peaks identification : introduction

To perform calibration, we need to identify structures of energy deposit within the electromagnetic spectra in both simulations and measurements



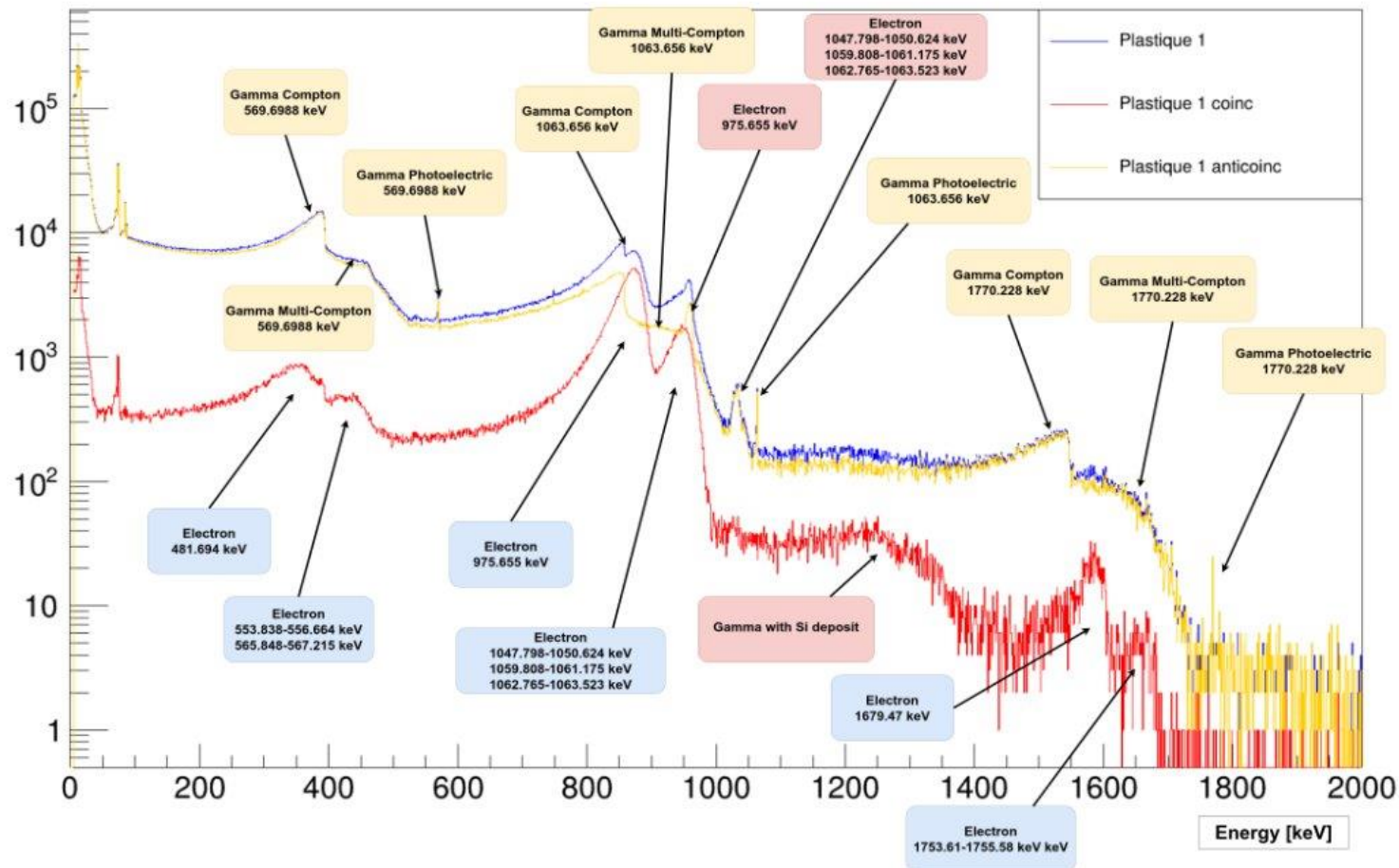
Once done it can be used to figure out the relation between energy and channels (energy calibration) and the relation between resolution and energy (resolution calibration)



Detectors calibration

Calibration peaks identification

Simulation Bi207 pl1



Identification of calibration peaks in nuclei/background spectra for each detector over ~0–8 MeV, accounting for peak merging and resolution effects.

CALIBRATION PEAKS USED SO FAR

- Fitting known structures both in measurements and simulation
- For γ rays in HPGe and CeBr₃ detectors, photopeaks were used whereas in plastic detectors compton edges were used due to their different energy deposit response
- Due to their design, silicon detector calibration was performed using only conversion electrons below 1.1MeV

	207Bi	40K	208Tl	98Nb	114Ag	91Rb	90Rb	96Y	92Rb
only for silicon detectors	c.e. 482	γ 1461	γ 2615	ep 4600	ep 5072	ep 5899	ep 6579	ep 7096	ep 8096
	c.e. 554-557					γ 94			
	γ 570					γ 346			
only for plastic and silicon	γ 1064					γ 439			
	c.e. 976					γ 593			
	c.e. 1047-1064					γ 603			
	γ 1770					γ 1137			
						γ 1616			
						γ 1971			
						γ 2564			
						γ 3147			
						γ 3600			
						γ 4078			

Note : Due to the design of the setup, plastic scintillators see mostly electrons with an emission energy higher than $\sim 400\text{keV}$ and for CeBr₃ $\sim 1600\text{keV}$,

only for HPGe and CeBr₃

only for CeBr₃

ep : endpoint
c.e. : conversion electron

Energy is in keV

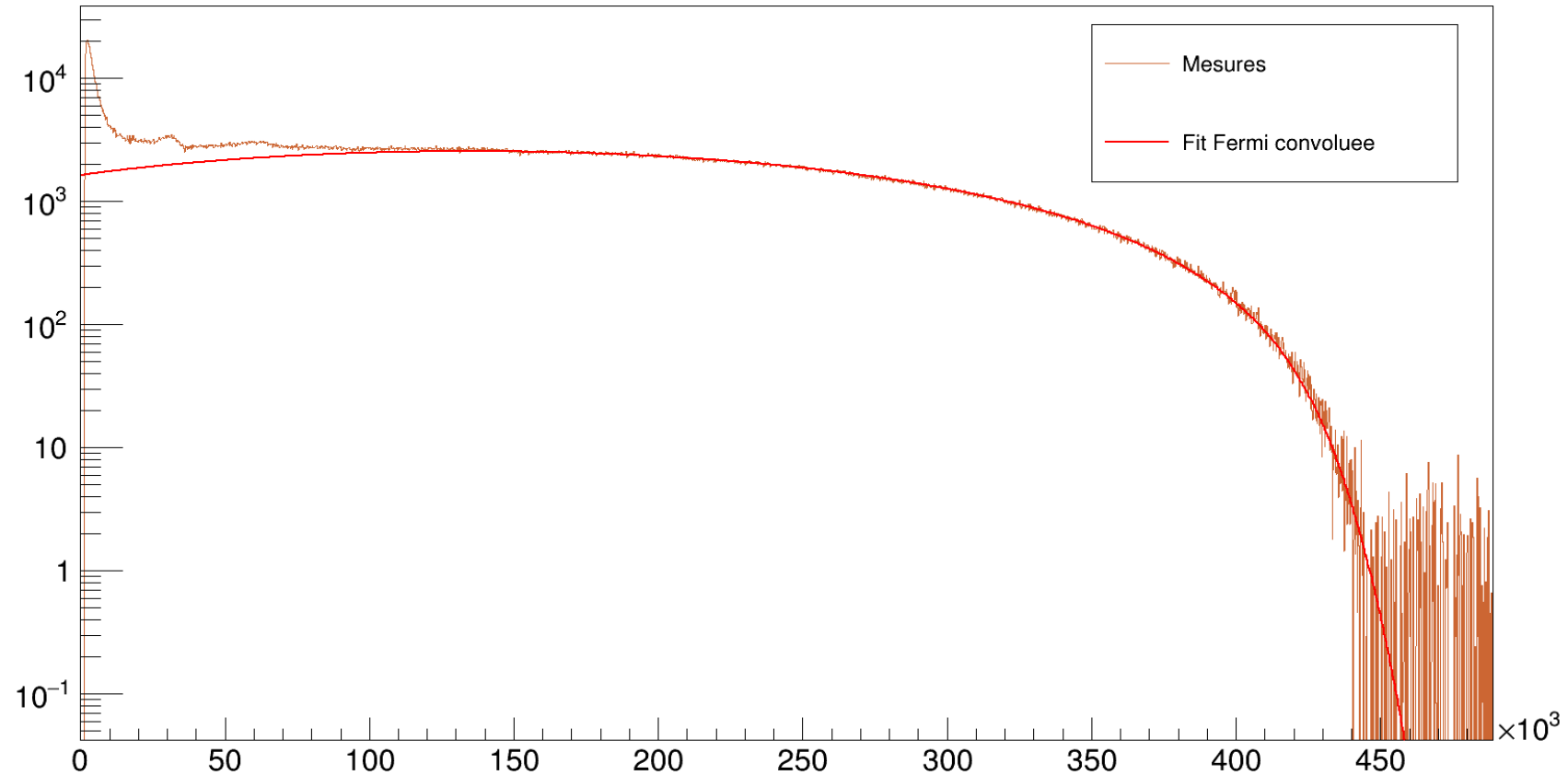
Detectors calibration

Fitting the calibration peaks

- Fitting known structure both in measurements and simulation
- Conversion electron
- Compton edge
- Photopeak
- Endpoint

- Functions used :
- Crystal Ball
- Gaussian
- Fermi function x Phase space

Endpoint fit on a ^{92}Rb measurement in Plastic scintillator



Detectors calibration

Resolution modeling

Independent C++ implementation of convolution code for gaussian resolution with analytical re-derivation

Convolved function = function * gaussian

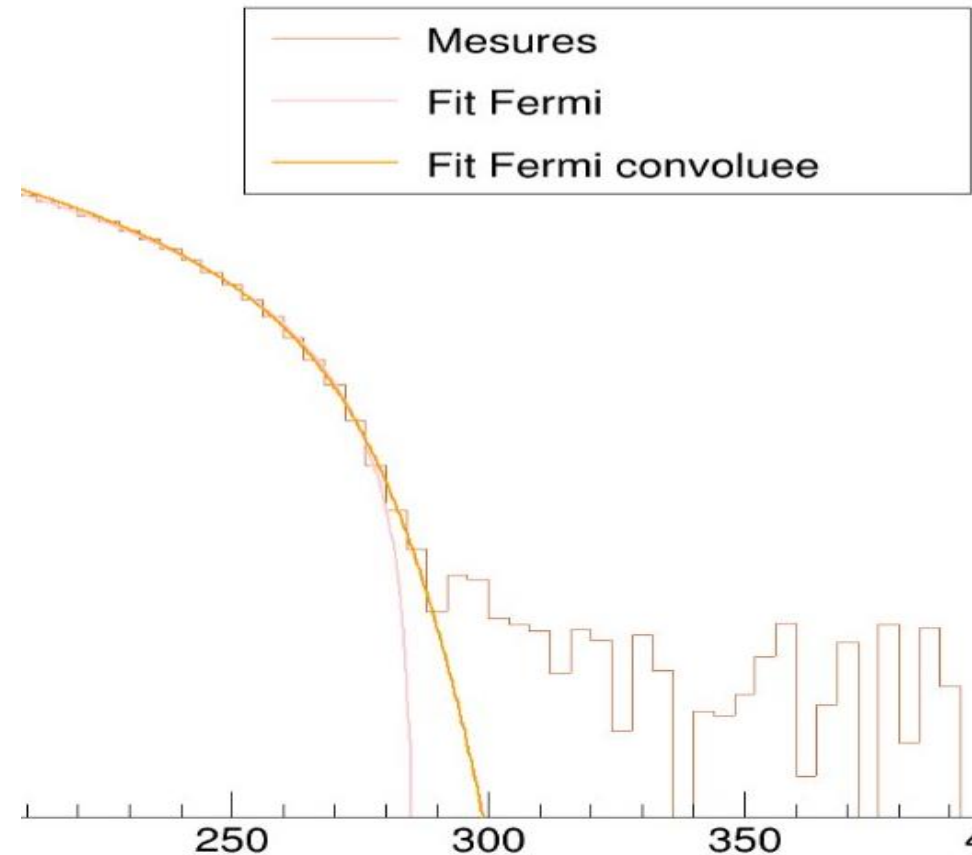
$$F[i] = (f * G)[i] = \sum_{j=-\infty}^{+\infty} f[j]G[i-j]$$

Can be applied to simulated spectra as well as fit functions

Standard endpoint fit



(Fermi function x Phase space) * Convolution -> Endpoint + Resolution informations 18

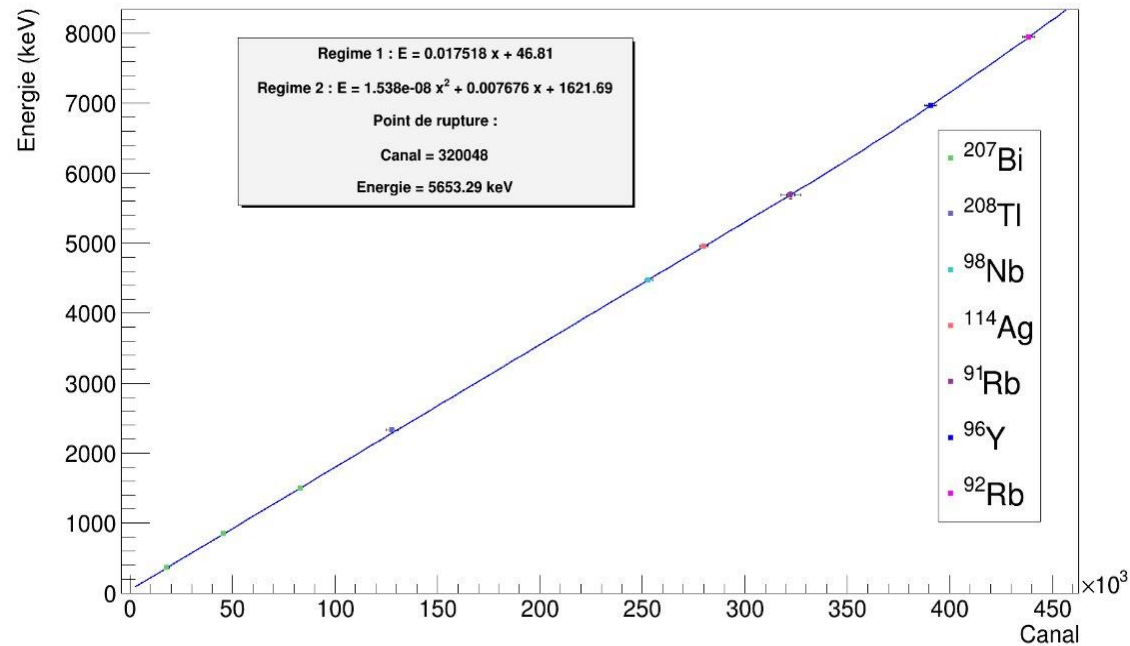


Detectors calibration

Calibration functions

Energy calibration function in Plastic scintillator 1

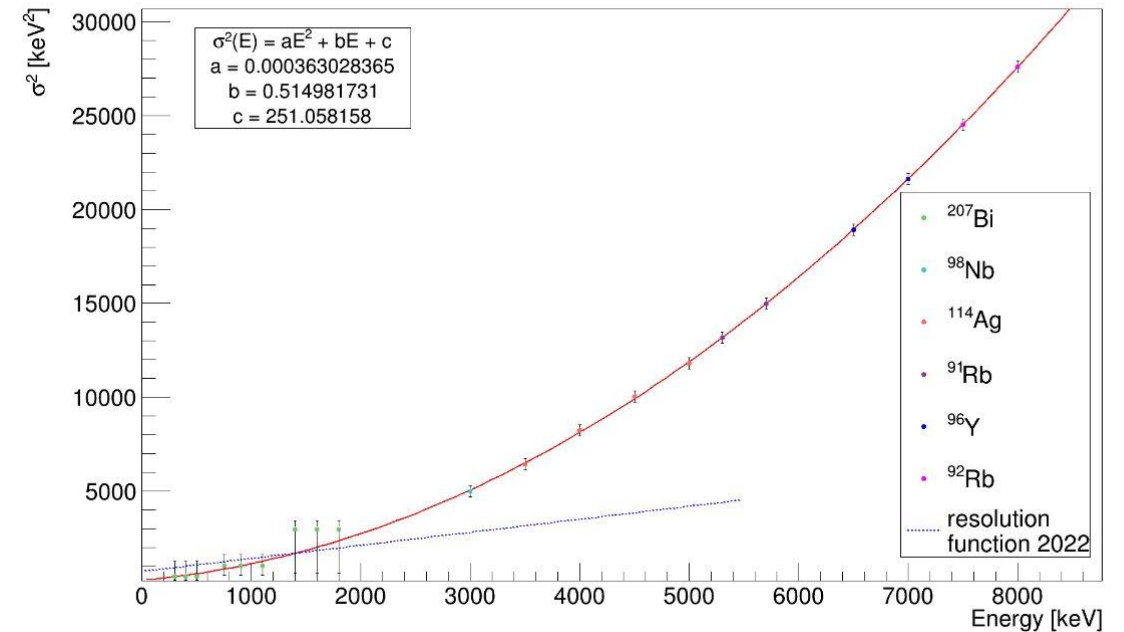
Fonction de calibration en energie PI1



Linear regime then quadratic regime

Energy resolution function in Plastic scintillator 1

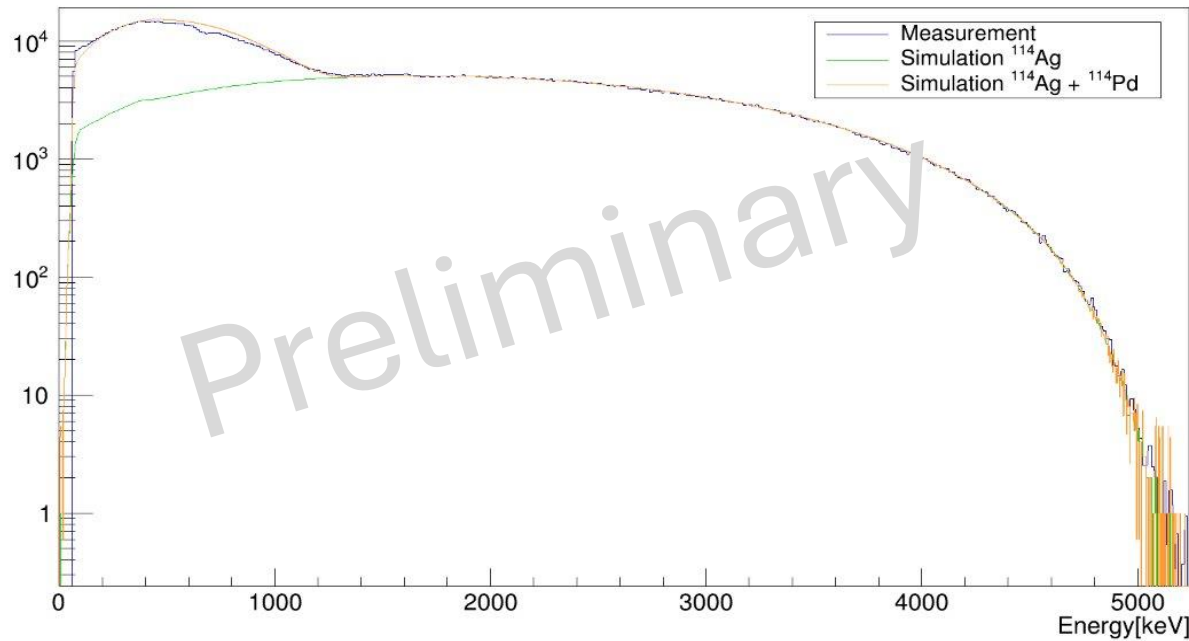
Energy resolution function PI1



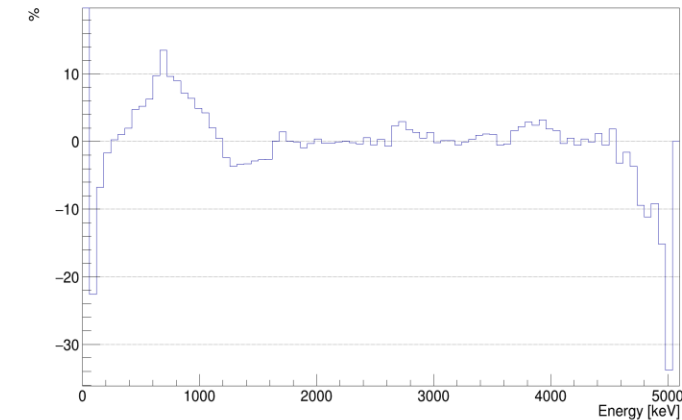
In 2022 : Linear function evaluated up to 2MeV
 My work: Quadratic function evaluated up to 8MeV

Data-Simulation comparison

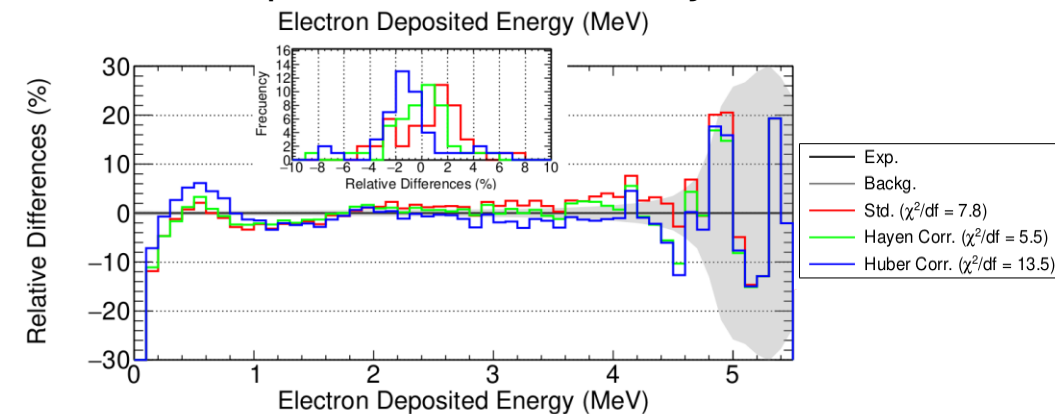
^{114}Ag PI1 coinc



Deviation ^{114}Ag coinc



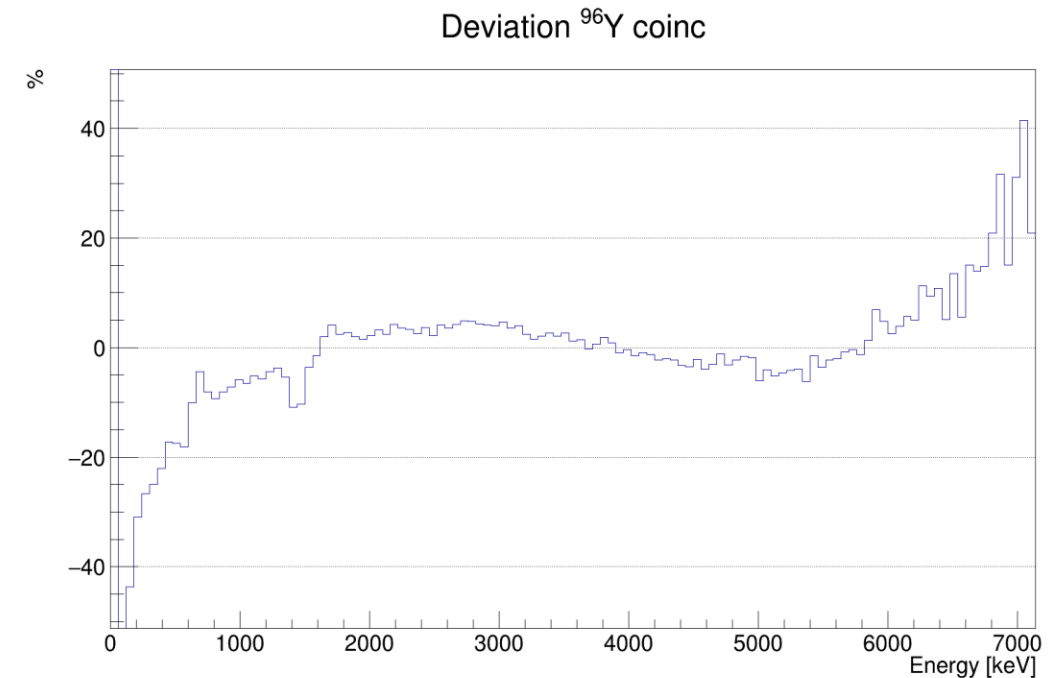
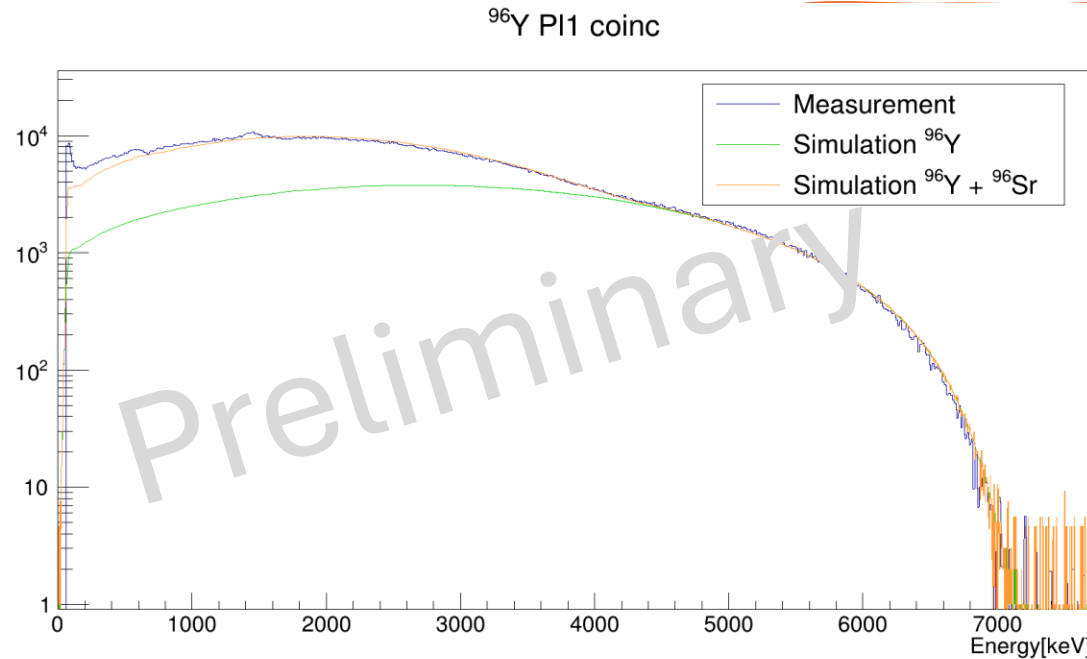
Comparable to 2022 analysis



-First validation of the simulation data reproduction
(below 5% of deviation)

-Still need to apply quantum corrections to the simulated spectra

Data-Simulation comparison



-Work in progress but a fair agreement is already obtained

-Some cases like ⁹⁶Y need TAGS data to be included in the event generator for better reproduction

-Still need to apply quantum corrections to the simulated spectra

Conclusion and Outlook

- Geometry of the detectors fully reproduced in GEANT4
- Convolution code and calibration techniques have been developed
- Detectors calibration have been performed through several radioactive nuclei spectra (still a work in progress)
- Application of corrections (and TAGS data when needed) to the event generator
- Detector response matrix
- Deconvolve the measured beta spectra
- ^{96}Y and ^{94}Y shape factors evaluation and comparison to theory predictions
- Include those shape factors to summation method

What have been done

Quite soon

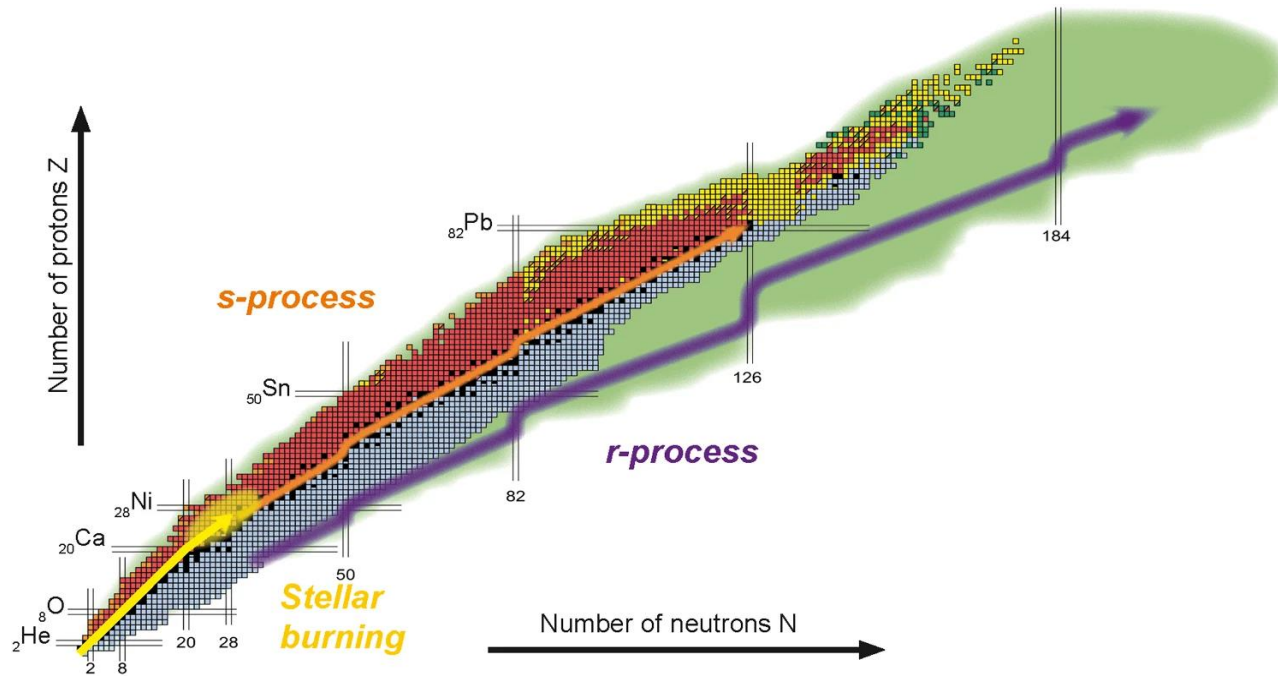
Near future

What's to be done

Final goal if we have time

Physics motivations

Nuclear astrophysics : r-process calculations



credit: EMMI, GSI/Different Arts

- The r-process synthesizes about half of the elements heavier than iron
- Beta decays govern the evolution of matter back toward stability
- Many r-process nuclei are expected to exhibit significant forbidden transitions contributions
- Improved beta decay modeling benefits both reactor antineutrino predictions and r-process calculations

